Numerical Analysis of the Contact Pressure in a Quasi-Static Elastomeric Reciprocating Sealing System

Serge Tsala
LaMCoS UMR CNRS5259/INSA-LYON,
20 Avenue Albert Einstein,
Villeurbanne Cedex 69 621, France;
Safran Landing Systems,
9 Rue Antoine de Saint-Exupéry,
Molsheim 67120, France

Yves Berthier
LaMCoS UMR CNRS5259/INSA-LYON,
20 Avenue Albert Einstein,
Villeurbanne Cedex 69 621, France

Guilhem Mollon
LaMCoS UMR CNRS5259/INSA-LYON,
20 Avenue Albert Einstein,
Villeurbanne Cedex 69 621, France

Aude Bertinotti
Safran Landing Systems,
9 Rue Antoine de Saint-Exupéry,
Molsheim 67120, France

In this technical brief, we present detailed finite element simulations of a sealing system operating in quasi-static conditions, in the framework of the real piston actuator of a landing gear braking system. Numerical results show two peaks of the contact pressure on the rod, and demonstrate that this contact pressure remains larger than that in the fluid chamber. These numerical results are qualitatively validated by scanning electron microscopy (SEM) observations of a worn sealing system. Overall, this study shows the benefits of numerical simulation in geometrical design of sealing systems targeting a given contact pressure at the rod/seal interface. [DOI: 10.1115/1.4040154]

Keywords: reciprocating sealing system, design methodology, elastomeric seal, contact pressure, reliability

1 Introduction

Reciprocating sealing systems are devices used as actuators in many industrial applications such as construction machines, production chains, and landing gear braking systems. Their reliability is essential for financial, ecological, and security reasons. A reciprocating sealing system is reliable when presenting a good sealing performance associated with a sufficient life expectancy. Tribological study of such systems began around the year 1930 [1].

Martin [2] defines the sealing as the performance in containment of the fluid inside an equipment. He classifies the sealing types into groups depending on the level of the leakage rate. According to Nikas [1], the mechanism of the sealing is related to the contact pressure distribution. The main goal of most studies is the quantification of fluid losses. Experimental studies focus on the development of experimental setup for the measurement of friction and the fluid flow quantification [3–5], while the numerical ones attempt to assess the fluid thickness in the contact and quantify the amount of leaking fluid [6]. No existing strategy seems to take into account the tribological triplet developed by Godet [7], while this approach has proved useful in a large number of other tribo-systems [8,9].

The design of a reciprocating sealing system is a complex task, which requires a great deal of expertise. It requires knowledge in materials science, tribology, manufacturing technology, production engineering, fluid engineering, chemistry, and physics, and an overall appreciation of engineering systems [10]. Accumulated studies to date have shown a great number of parameters affecting the performance of a sealing system, but it appears that most of them are somewhat related to the contact pressure distribution, as predicted by Nikas [1]. The present technical note intends to contribute to this issue by proposing a precise numerical simulation of a sealing system, aiming at the assessment of the contact pressure distribution in the case of quasi-static operating conditions. For illustrative purpose, the design of the piston actuator of a landing gear braking system will be used as a case of application.

The large amount of sealing parameters available in the literature [11,12] illustrates the great work done to overcome the sealing problem. But, there are so many parameters that it is difficult for the designer to take all of them into account. Indeed, they are usually presented without any link between them and without any existing methodology intended to determine them. The fact that all the sealing parameters are related in some way to the contact pressure means that this quantity can be defined as a signature of the sealing mechanism and considered as the main parameter for the design of the piston. In quasi-static conditions, common practice states that for a "rigorous sealing" performance [2], in a reciprocating seal, the contact pressure (P_c) should be greater than the fluid pressure (P_f) [13,14]

$$P_c > P_f \tag{1}$$

This criterion is applied on piston actuators of landing gear braking systems (Fig. 1). The sealing system is composed of a rod at the center of the piston, a seal, and an anti-extrusion ring. The piston operates as a single acting cylinder containing a spring, which ensures the instroke of the piston. The fluid used in the system is a phosphoric ester at room temperature. The material of the seal is an éthylene-propylene-diene monomer and that of the anti-extrusion ring is a polytetrafluoroethylene.

The system operates in quasi-static conditions with an average speed of the seal below 1 mm/s during the outstroke. The low sliding velocity of the seal precludes both inertial effects in the mechanisms and dynamic pressure build-up in the possible interfacial fluid. During the braking phase, the hydraulic pressure reaches 12 MPa. This phase is preceded by the outstroke and followed by the instroke. Section 2 will present the numerical simulations followed by an experimental validation. The reciprocating system of the hydraulic piston is illustrated in Fig. 2.

2 Numerical Simulation

An axisymmetric model of the system was developed and implemented in the software ABAQUS EXPLICIT, due to severe nonlinearities in the problem (frictional contacts, material constitutive law, and large displacements). A moderate mass scaling is used in order to accelerate the simulation without disturbing it (thanks to the very limited contribution of inertial effects to the mechanical behavior of the system). The model is presented in Fig. 3. The rod diameter is about 6 mm. The simulation is performed in three steps. At the beginning, the radius of the seal is larger than the allowed space between the rod and the piston (see Fig. 3). The first and second steps are dedicated to the assembly of the seal. The first step is a radial compression of the seal and the second one is a relaxation of the seal so that we obtain a surface to surface contact between the rod and the seal on one side and the seal and the piston on the other. The seal is tight at this position and its deformation generates a residual contact pressure on the rod. In

Contributed by the Tribology Division of ASME for publication in the JOURNAL OF TRIBOLOGY. Manuscript received December 10, 2017; final manuscript received April 24, 2018; published online May 21, 2018. Assoc. Editor: Noel Brunetiere.

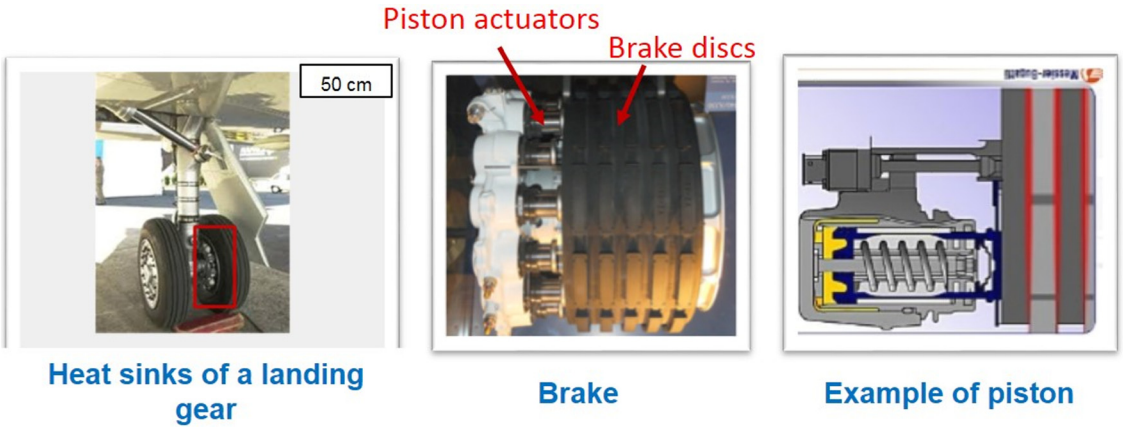

Fig. 1 Piston actuator of a landing gear braking system

step 3, the hydraulic pressure applied on the fluid side of the seal triggers the motion of the piston with the compression of the spring. This motion is stopped by the brake disks resistance illustrated here by the final position of the piston. During the instroke, the hydraulic pressure decreases and the motion of the piston is ensured by the relaxation of the spring.

In this model, the rod and the brakes (final position of the piston) are fixed, and the piston, the seal, and the anti-extrusion ring are free of any imposed displacement (although the axisymmetric nature of the model largely constrains their motions). The piston and the rod are made of steel modeled as a linearly elastic material. The elastomeric seal is in éthylene-propylene-diene monomer, modeled as a Mooney–Rivlin hyperelastic material as it has been found suitable according to the related literature [1], of parameters $C_{10} = 1.45$, $C_{01} = 0.45$, and $D_1 = 0.011$ and a density of $900\,\text{kg/m}^3$. The friction coefficients used to perform the simulation are presented in Fig. 4. A penalty contact method is used to perform the simulation. Since this study aims at assessing the contact pressure within the seal–rod interface, the possible presence of a fluid is not taken into account explicitly in the simulations. As usually done in similar studies [15–17], it is only considered by the means of the friction coefficient. The complex question of the appropriate value for this coefficient, depending on the lubrication regime, cannot be tackled with a model at the scale of the whole system, and is left for further studies.

The element types used to mesh the parts are four-node reduced-integration, axisymmetric, solid element noted CAX4R, except for the elastomeric seal composed with CAX4R and CAX3, which is a three-node linear element, to allow some large deformations in the seal. The total number of nodes is about 33,000 and the shortest element size is about 5 μm. An analysis of the mesh dependency of the model was performed in order to ensure its accuracy (Fig. 5). Most of the computational burden lies in the refined contact zones of the seal and of the anti-extrusion ring.

The developed model performs a stable resolution for hydraulic pressures up to 20 MPa. The evolution of the hydraulic pressure in time during the operating phases is presented in Fig. 6. This figure shows that the hydraulic pressure reaches 12 MPa during the braking phase. On the same figure, the speed variation of a seal point O (Fig. 5) located at the inner zone of the interface gives an idea of the seal motion on the rod. During the instroke phase, the seal starts to slip at time A and reaches its final position at time B (although the maximum fluid pressure is not reached yet), and during the outstroke phase, it slides from times C to D (Fig. 6).

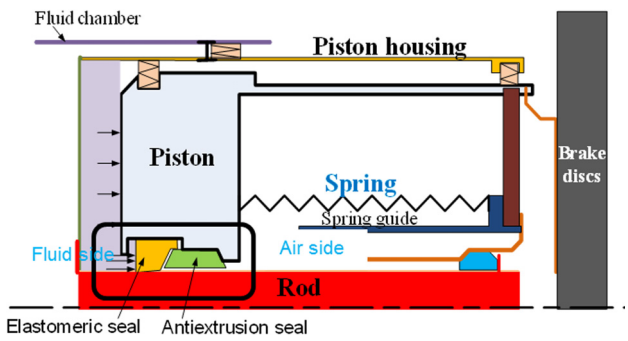

Fig. 2 Axisymmetric illustration of the piston actuator

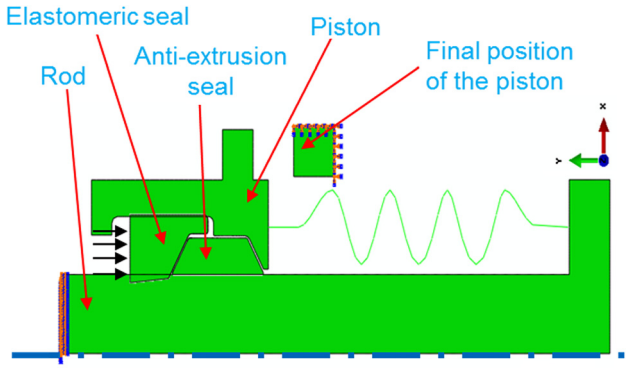

Fig. 3 Axisymmetric model of the piston in ABAQUS 6.12

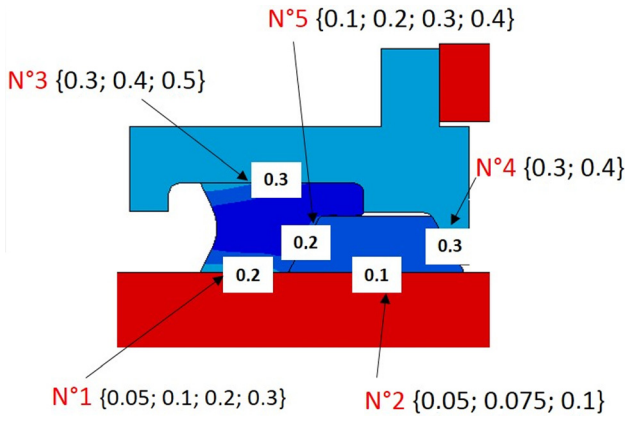

Fig. 4 Coefficient of friction at different interfaces; in brackets: range of the values tested in the parametric study; in white rectangles: reference value

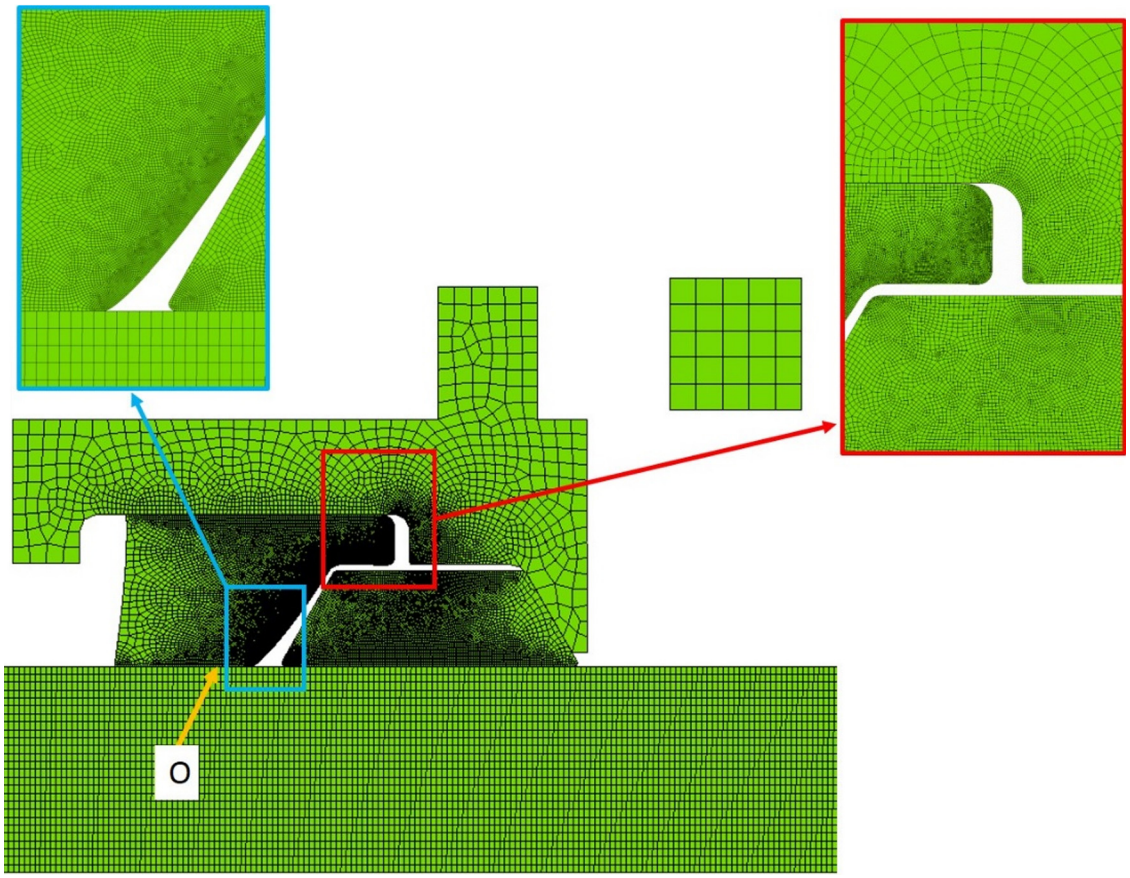

Fig. 5 Illustration of the meshed model

The deformed shape of the seal and the rod/seal contact pressure are presented in Fig. 7. The pressure applied by the fluid on the left-hand side of the elastomeric seal induces a deformation which generates a contact pressure at the rod/seal interface. This contact pressure depends on the operating phase, as shown in Fig. 7. This figure also demonstrates that the rod/seal contact pressure is larger than the hydraulic pressure at two peaks during the braking phase. This observation holds through the entire loading cycle. The first peak is on the fluid side and the second one on the anti-extrusion side. The seal design is thus in agreement with the sealing criterion of Eq. (1), and both geometry and materials were chosen adequately.

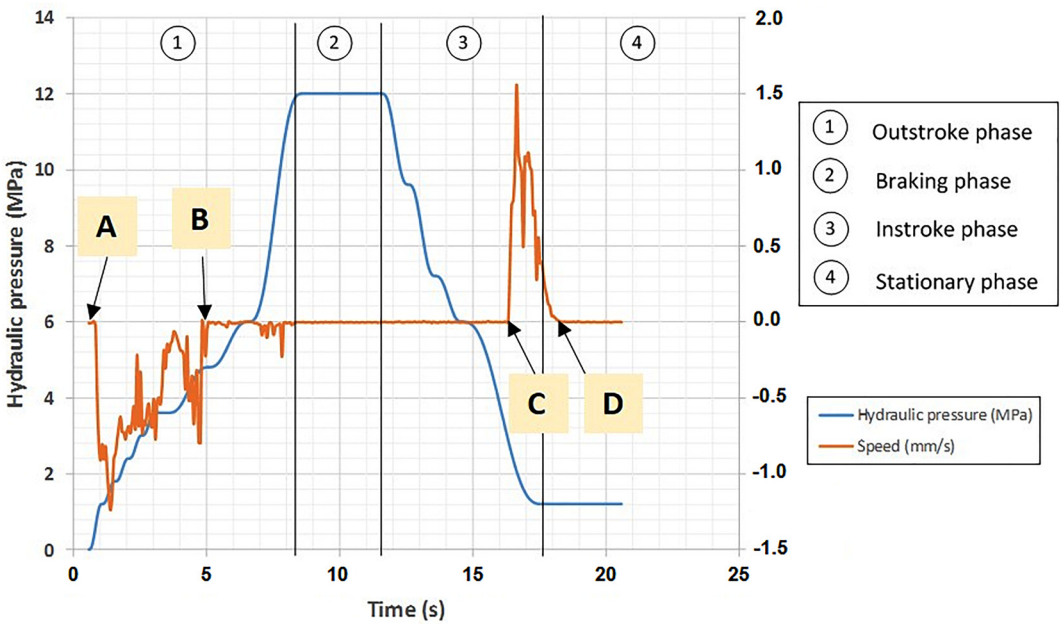

Fig. 6 Evolution of the hydraulic pressure and sliding speed of the seal

3 Qualitative Experimental Validation

An scanning electron microscopy (SEM) observation is performed on samples of real pistons after more than 140,000 cycles. The texture of used samples is compared with the texture of a new seal. During the operating phase, wrinkles observed at the surface of a new seal are detached under the effect of the contact pressure and become the third body at the rod/seal interface. Then, the contact pressure peaks observed in simulations on both extremities of the rod/seal interface are consistent with the smooth texture observed in pictures a and c of SEM observations (Fig. 8). These locations can be associated with a larger degradation of the interface materials, triggering third body generation. In contrast, the low contact pressure area at the inner zone of the seal explains the particles accumulation observed in picture b (Fig. 8). It can be postulated from these evidences that it is difficult for a particle to cross a contact pressure peak. Thus, a possible interpretation is that both peaks play the role of a third body barrier, especially as those peaks exist during all the operating phases. Validating this assumption is not an easy task, and might require some fine modeling of the behavior of the third body in the presence of a pressure gradient during reciprocating slip, using such techniques as discrete element modeling [8,9,18] or a multibody mesh-free approach [19]. Besides, a large change in the seal geometry might affect the pressure distribution, although this would require a catastrophic wear associated with the expulsion of a large amount of third body out of the contact. Given the low stiffness of the seal compared to the applied pressure, this is regarded as an accidental phenomenon which is out of the scope of the present study. Hence, in the current state of our knowledge, it appears that the numerical model provides results, which are consistent with the experimental observations. It provides some understanding of the wear process at the rod–seal interface, and demonstrates that the seal design is correct.

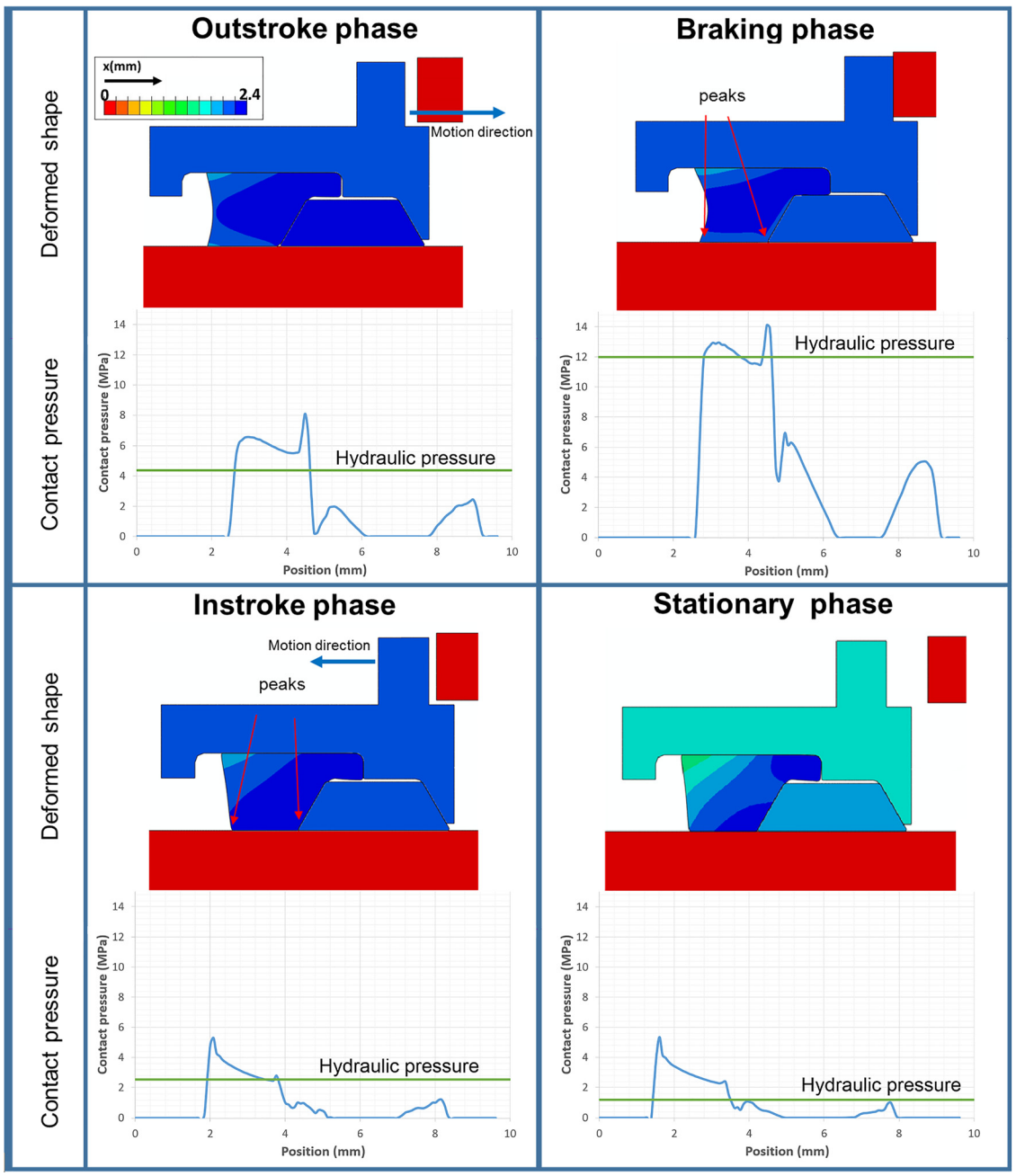

Fig. 7 Summary of the simulation results

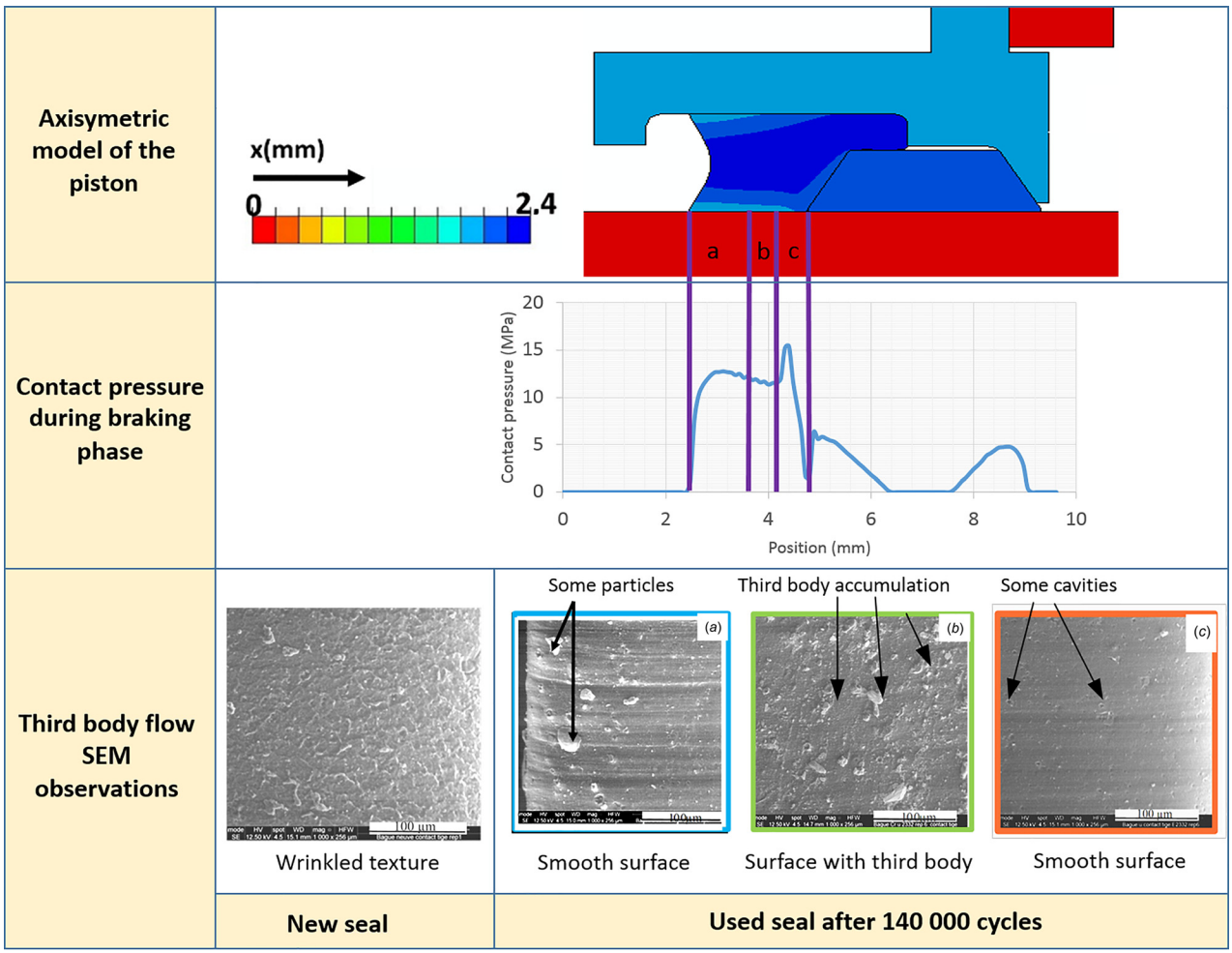

Fig. 8 Experimental validation of the numerical design

4 Parametric Study

4.1 Influence of the Seal Stiffness. The influence of the seal stiffness on the contact pressure is studied here. The elastomeric material constitutive law is defined by the strain energy density function for an incompressible Mooney–Rivlin model by [20]

$$W(I_1, I_2) = C_{10}(I_1 - 3) + C_{01}(I_2 - 3) \tag{2}$$

Where C_{01} and C_{10} are material constants (determined based on appropriate mechanical testing on elastomer samples), and I_1 and I_2 are the first and the second invariants of the left Cauchy–Green deformation tensor. Then, the Young's modulus at zero deformation is defined as

$$E_0 = 6(C_{01} + C_{10}) \tag{3}$$

It characterizes the stiffness of the elastomeric material. The Young's modulus at zero deformation is used here to differentiate elastomeric materials. A comparison of the influence of the stiffness of the elastomer on the contact pressure is studied in this paragraph. Results are shown in Fig. 9 for four materials.

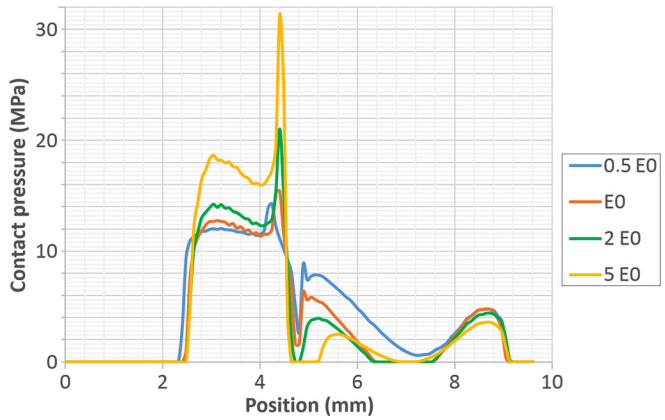

Fig. 9 Evolution of the rod/seal contact pressure during the braking phase with the stiffness of the seal

For all the cases studied here, the threshold pressure of 12 MPa is achieved, but it appears that the stiffer the elastomeric material is, the easier it is to achieve the threshold contact pressure.

On the other hand, the increase in the stiffness of the seal results in a high pressure peak at the front of the seal. This area could be subject to rapid third body generation. This observation indicates that although it is better to have a high stiffness for the seal material, there is a maximum allowable Young's modulus value for the seal material.

4.2 Influence of the Friction Coefficients. This parametric study aims to evaluate the influence of the friction coefficients at each interface of the system on the contact pressure at the rod/seal interface. Five interfaces do exist in the numerical model of the hydraulic piston shown in Fig. 4. For the influence of the rod/seal interface, four values of friction coefficient are tested, and the results are illustrated in Fig. 10.

The deformed shape in Fig. 10 presents the displacement field in the axial direction of the piston. The figure shows that the radius of curvature at the fluid side of the seal decreases when the friction coefficient increases. In fact, the sliding at the interface for elastomeric material is always in competition with the volumetric shear of the bulk so as to be able to accommodate the relative motion of the piston and of the rod. In this model, the friction coefficient is constant at the seal/housing interface. It clearly appears that an increase of the friction on the rod/seal interface reduces the slip and generates an increased bulk shear in the seal,

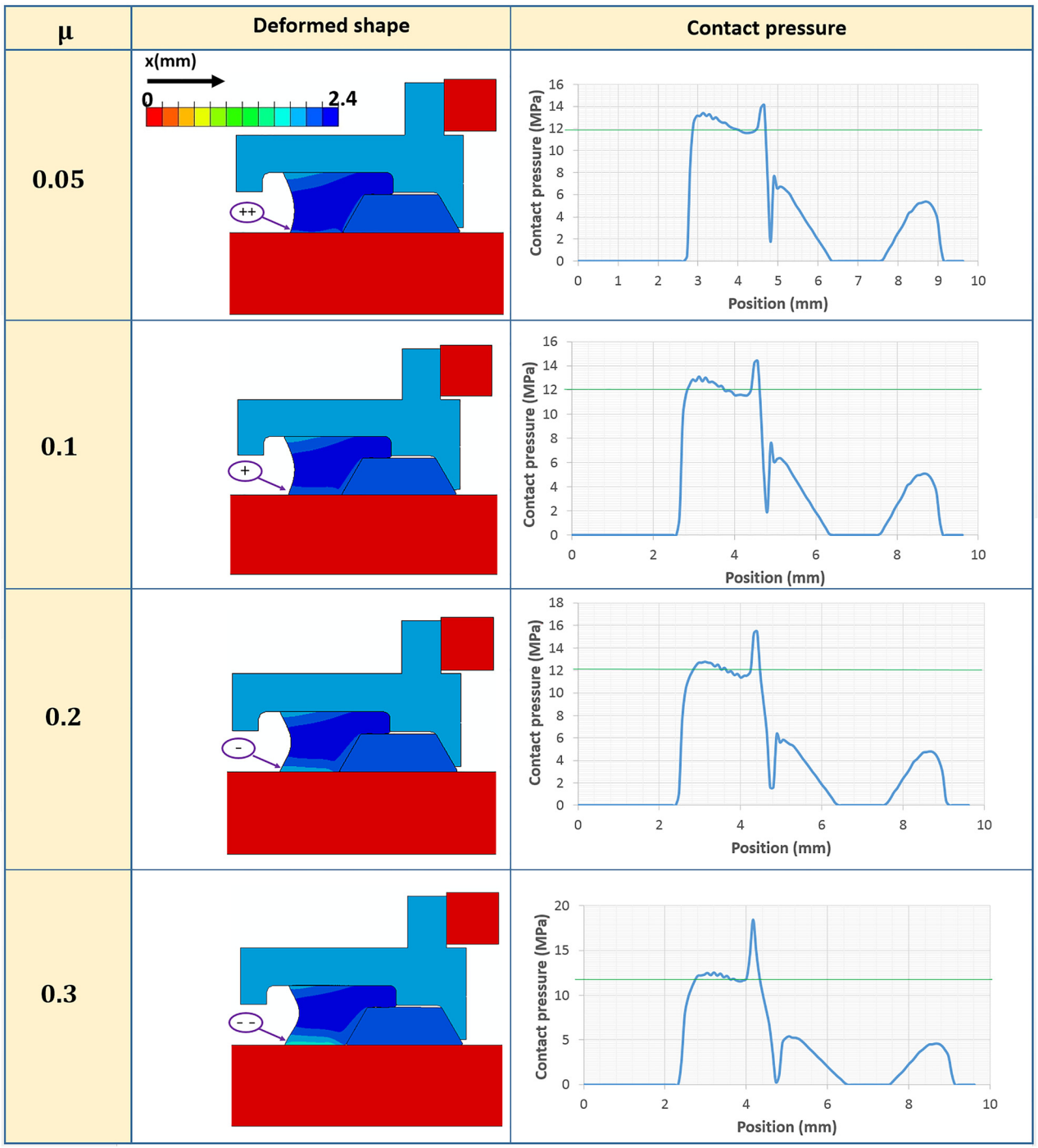

Fig. 10 Evolution of the deformed shape and the contact pressure during the braking phase with the friction coefficient

Table 1 Evolution of the rod/seal contact length with the friction coefficient during the braking phase

Friction coefficient	0.05	0.1	0.2	0.3
Rod/seal contact length (mm)	2.11	2.17	2.43	2.59

modifying the profile of contact pressure within the interface. The slip ability of the seal at the rod/seal interface is illustrated in the figure from "++" to "− −." It results in a gradual increase of the rod/seal contact length with the friction coefficient as illustrated in Table 1.

Additional simulations with varying friction coefficient at the other interfaces (seal/housing, seal/anti-extrusion ring, housing/anti-extrusion ring, and rod/anti-extrusion ring, see Fig. 4) revealed that these friction coefficients do not affect the rod/seal contact pressure in a significant way.

5 Conclusion

In this paper, we proposed a modeling of a real reciprocating sealing system. We investigated the contact pressure at the rod–seal interface, by considering as a simplified design factor that this pressure must remain larger than that within the fluid chamber, as recommended in common practice. Numerical results showed that the pressure profile on the rod has two peaks (with varying intensities depending on the loading stage), and that the design criterion is met in all cases. The numerical results were qualitatively validated by SEM observations of a real system, where the localization of the third body deposits was found in good accordance with the numerical results. The study highlights the benefits of numerical simulation in the early stages of the design of sealing systems, in order to optimally determine the appropriate geometry and materials in order to meet the contact pressure design criterion. It also stresses the need of more local models in order to understand the behavior of the third body in the presence of a gradient of contact pressure during reciprocating slip.

Acknowledgment

The authors acknowledge the French National Association of Research and Technology (ANRT) for its financial support to this Work through the CIFRE convention No. 2013/0939, in collaboration with the company Safran Landing Systems, which is also gratefully acknowledged.

References

[1] Nikas, G. K., 2010, "Eighty Years of Research on Hydraulic Reciprocating Seals: Review of Tribological Studies and Related Topics Since the 1930s," Proc. Inst. Mech. Eng. Part J, **224**(1), pp. 1–23.
[2] Martin, J., 2004, "Etanchéité en mécanique," Techniques de l'ingénieur Guidage mécanique, b5420, Editions T.I., Paris, France.
[3] Field, G. J., and Nau, B. S., 1973, "Film Thickness and Friction Measurements During Reciprocation of a Rectangular Section Rubber Seal Ring," Sixth BHRA International Conference on Fluid Sealing, Munich, Germany, Feb. 27–Mar. 2.
[4] Rana, A. S., and Sayles, R. S., 2005, "An Experimental Study on the Friction Behaviour of Aircraft Hydraulic Actuator Elastomeric Reciprocating Seals," Tribol. Interface Eng. Ser., **48**, pp. 507–515.
[5] Hörl, L., Haas, W., and Nißler, U., 2009, "A Comparison of Test Methods for Hydraulic Rod Seals," Sealing Technol., **2009**(12), pp. 8–13.
[6] Salant, R. F., Maser, N., and Yang, B., 2007, "Numerical Model of a Reciprocating Hydraulic Rod Seal," ASME J. Tribol., **129**(1), pp. 91–97.
[7] Godet, M., 1984, "The Third-Body Approach: A Mechanical View of Wear," Wear, **100**(1–3), pp. 437–452.
[8] Kounoudji, K. A., Renouf, M., Mollon, G., and Berthier, Y., 2016, "Role of Third Body on Bolted Joints' Self-Loosening," Tribol. Lett., **61**(3), pp. 1–8.
[9] Rivière, J., Renouf, M., and Berthier, Y., 2015, "Thermo-Mechanical Investigations of a Tribological Interface," Tribol. Lett., **58**(3), pp. 48–59.
[10] Flitney, R., 2014, *Seals and Sealing Handbook*, Butterworth-Heinemann, Oxford, UK.
[11] Kanters, A. F. C., 1990, "On the Calculation of Leakage and Friction of Reciprocating Elastomeric Seals," Techishe Universiteit Eindhoven, Eindhoven, The Netherlands.
[12] Dipl, B., Papatheodorou, T., and Hannifin, P., 2005, "Influence of Hard Chrome Plated Rod Surface Treatments on Sealing Behavior of Hydraulic Rod Seals," Sealing Technol., **2005**(4), pp. 5–10.
[13] Ho, X. J., 2013, "Analyse De La Transmission Des Sollicitations Tribologiques Dans Un Presse-Garnitures De Robinet Pour En Maîtriser L'effort De Manœuvre Et L'étanchéité," Ph.D. thesis, INSA, Lyon, French.
[14] Ochoński, W., 1988, "Radial Stress Distribution and Friction Forces in a Soft-Packed Stuffing-Box Seal," Tribol. Int., **21**(1), pp. 31–38.
[15] Békési, N., and Varadi, K., 2010, "Wear Simulation of a Reciprocating Seal by Global Remeshing," Period. Polytech., Mech. Eng., **54**(2), pp. 71–75.
[16] Béséki, N., Vanadi, K., and Felhos, D., 2011, "Wear Simulation of a Reciprocating Seal," ASME J. Tribol., **133**(3), p. 031601.
[17] Zhang, H., and Zhang, J., 2016, "Static and Dynamic Sealing Performance Analysis of Rubber D-Ring Based on FEM," J Failure Anal. Prev., **16**(1), pp. 165–172.
[18] Mollon, G., 2015, "A Numerical Framework for Discrete Modelling of Friction and Wear Using Voronoi Polyhedrons," Tribol. Int., **90**, pp. 343–355.
[19] Mollon, G., 2018, "A Unified Framework for Rigid and Compliant Granular Materials," Comput. Part. Mech., epub.
[20] Ali, A., Fouladi, M. H., and Sahari, B., 2010, "A Review of Constitutive Models for Rubber-Like Materials," Am. J. Eng. Appl. Sci., **3**(1), pp. 232–239.